

## In Situ Construction of a Coordination Zirconocene Tetrahedron

Guoliang Liu,<sup>†,‡</sup> Zhanfeng Ju,<sup>†</sup> Daqiang Yuan,<sup>\*,†</sup> and Maochun Hong<sup>†</sup><sup>†</sup>State Key Laboratory of Structural Chemistry, Fujian Institute of Research on the Structure of Matter, Chinese Academy of Sciences, Fuzhou, 350002 Fujian, People's Republic of China<sup>‡</sup>University of Chinese Academy of Sciences, Beijing 100049, People's Republic of China

## Supporting Information

**ABSTRACT:** The current study describes the first in situ synthesis and characterization of a new family of cationic coordination tetrahedra of both the  $V_4F_4$  and  $V_4E_6$  type, which are constructed by a new building block based on a trinuclear zirconocene moiety and the dicarboxylate or tricarboxylate anions.

The self-assembled coordination polyhedra have received much attention from chemists and not only illustrate the beauty of chemistry and art of synthesis but also reveal potential applications at the frontiers of chemistry and materials science.<sup>1</sup> As the simplest Platonic polyhedron, coordination tetrahedra are very important because of their abilities as catalysts for chemical transformations, mimics of the microenvironments of bioprocesses, and stabilization of reactive intermediates and metastable materials.<sup>2</sup> Although the fundamental concepts of constructing a coordination tetrahedron are well understood,<sup>3</sup> the rational design and synthesis of a new coordination tetrahedron is still filled with challenges. Usually, the cyclopentadienyl or arene metal moiety can be used to build up supramolecular architectures.<sup>4</sup> However, they have never been extensively employed to generate coordination tetrahedra. In this work, we report a series of robust coordination tetrahedra that are assembled by a zirconocene unit and carboxylate acid. To the best of our knowledge, it is first reported that the isostructural supramolecular structures of the coordination tetrahedra have been prepared with zirconocene nodes in a one-step in situ method.

Bis(cyclopentadienyl)zirconium dichloride ( $Cp_2ZrCl_2$ ,  $Cp = \eta^5-C_5H_5$ ) can be slowly hydrolyzed in water and carboxylate acid to form a trinuclear ligand-bridged ( $C_5H_5$ ) $Zr$ -cation cluster (Figure 1a).<sup>5</sup> The trinuclear cluster is close to  $C_3$  symmetry with the carboxylate ligands oriented to one face and the  $\mu$ -OH groups oriented to the other, in which the  $C_2$  axes in carboxylate ligands form an angle of about  $60^\circ$ . Thus, the trinuclear cluster looks like a 3-connected secondary building unit (SBU) with pyramidal geometry and provides a chance to use it as a vertex to construct coordination polyhedra. One of the simplest strategies is the replacement of the original carboxylate in the SBUs by the linear dicarboxylate, which will easily form a  $V_4E_6$  ( $V =$  vertex and  $E =$  edge) coordination tetrahedron (Figure 1b). Meanwhile, a  $V_4F_4$  ( $F =$  face) coordination tetrahedron will be created under proper trigonal tricarboxylate conditions. With this background in mind, we attempted the assembly of a coordination tetrahedron based on zirconocene nodes and ditopic or tritopic carboxylate ligands.

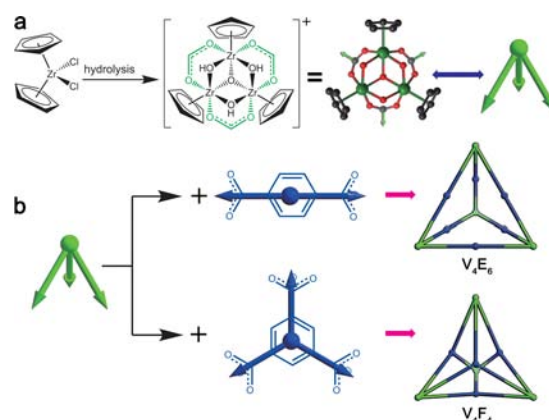


**Figure 1.** (a) Schematic representations of the formation of trinuclear zirconocene nodes. (b) Configurations of  $[4 + 6] V_4E_6$  and  $[4 + 4] V_4F_4$  tetrahedra.

The reaction of  $Cp_2ZrCl_2$  and benzene-1,4-dicarboxylic acid ( $H_2BDC$ ) in the mixtures of  $N,N$ -dimethylformamide (DMF) and  $H_2O$  at  $60^\circ C$  for 8 h resulted in the isolation of single crystals of the complex  $\{[Cp_3Zr_3O(\mu_2-OH)_3]_4(BDC)_6\} \cdot Cl_4 \cdot nS$  (**1**, where  $S =$  noncoordinated solvent molecule). Just as expected, the single-crystal X-ray structure of **1** revealed that an isolated cationic coordination zirconocene tetrahedron,  $\{[Cp_3Zr_3O(OH)_3]_4(BDC)_6\}^{4+}$  ( $ZrT-1$ ), with  $V_4E_6$  topology was formed (Figure 2a), and the cationic charge was balanced by  $Cl^-$  (space group  $I4_1/a$ ). The vertices of  $ZrT-1$  are composed of  $Cp_3Zr_3O(OH)_3$  SBUs, in which the  $Cp$  ligands block one coordination site of  $Zr$  atoms to prevent the formation of extended structures. The edges of  $ZrT-1$  are occupied by six ditopic  $BDC$  ligands.  $ZrT-1$  has ideal  $S_4$  symmetry with one-fourth of the coordination tetrahedron (one SBU and one and half ligands) appearing in the asymmetric unit. In  $ZrT-1$ , the separation of  $\mu_3-O \cdots \mu_3-O$  is about  $11.0 \text{ \AA}$ , and the internal tetrahedral volume is about  $158 \text{ \AA}^3$ , estimated using the *VOLCAL* program in the *WinGX* package (Table S2 in the Supporting Information, SI). In the crystal, one tetrahedron is connected to four adjacent tetrahedra through double  $O-H \cdots Cl \cdots H-O$  hydrogen bonds (Figure S1a in the SI) to form a porous material that shows 44.9% porosity calculated using the *PLATON* routine with a probe radius of  $1.8 \text{ \AA}$ .<sup>6</sup> The connection between the tetrahedra is approximately considered as a vertex-sharing mode, which results in a 3-fold interpenetrated

Received: September 25, 2013

Published: November 26, 2013

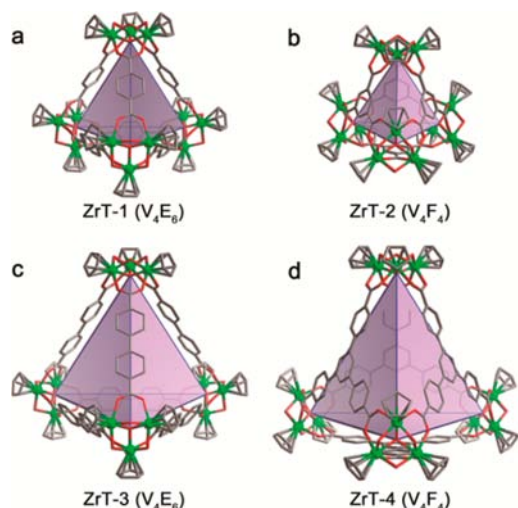


**Figure 2.** Crystal structures of cationic coordination zirconocene tetrahedra. Color code: C, gray; O, red; Zr, green. The free spaces in the coordination tetrahedra are depicted as the inserted pink tetrahedra. For clarity, H atoms were omitted.

diamondoid topology if the tetrahedron is regarded as a node (Figure S1b in the SI). The severely disordered solvent molecules can hardly be located from the single-crystal X-ray diffraction data, which may be both inside and outside ZrT-1. On the basis of elemental analysis and thermogravimetric analysis (TGA), the as-synthesized **1** contained 47 DMF and 90 H<sub>2</sub>O molecules per unit cell.

Replacement of the BDC ligand by benzene-1,3,5-tricarboxylic acid (H<sub>3</sub>BTC) led to the formation of a new complex, {[Cp<sub>3</sub>Zr<sub>3</sub>μ<sub>3</sub>-O(μ<sub>2</sub>-OH)<sub>3</sub>]<sub>4</sub>(BTC)<sub>4</sub>}-Cl<sub>4</sub>·4DMF·*n*S (**2**). Complex **2** crystallizes in the tetragonal system (space group *P*<sub>4</sub><sub>2</sub>/*n*) and also features an isolated cationic coordination tetrahedron with chemical composition of {[Cp<sub>3</sub>Zr<sub>3</sub>μ<sub>3</sub>-O(μ<sub>2</sub>-OH)<sub>3</sub>]<sub>4</sub>(BTC)<sub>4</sub>}<sup>4+</sup> (ZrT-2). Unlike ZrT-1, ZrT-2 is a V<sub>4</sub>F<sub>4</sub> assembly with *T*<sub>d</sub> symmetry, in which the BTC ligands act as the faces of the tetrahedron (Figure 2b). The size of ZrT-2 is slightly smaller than that of ZrT-1; namely, the distance between two μ<sub>3</sub>-O molecules is 8.75 Å, and the calculated internal tetrahedral volume is about 79.2 Å<sup>3</sup>. Similar to crystal **1**, complex **2** forms a porous 2-fold interpenetrated diamondoid net by the similar double O—H...Cl...H—O hydrogen bonds observed in **1** (Figure S2 in the SI), and the evaluated value of the porosity is 44.5%, which includes 30 DMF and 35 H<sub>2</sub>O molecules per unit cell.

According to the basic principles of reticular chemistry, the extended carboxylate ligands are used to explore the construction of a coordination tetrahedron. Although the reaction conditions have not been completely optimized, coordination tetrahedra can be easily obtained using the aforementioned facile methods. As expected, two isorecticular complexes, {[Cp<sub>3</sub>Zr<sub>3</sub>μ<sub>3</sub>-O(μ<sub>2</sub>-OH)<sub>3</sub>]<sub>4</sub>(BPDC)<sub>6</sub>}-Cl<sub>4</sub>·*n*S (**3**) and {[Cp<sub>3</sub>Zr<sub>3</sub>μ<sub>3</sub>-O(μ<sub>2</sub>-OH)<sub>3</sub>]<sub>4</sub>(BTB)<sub>4</sub>}-Cl<sub>4</sub>·*n*S (**4**), were successfully synthesized with 4,4'-biphenyldicarboxylic acid (H<sub>2</sub>BPDC) and 4,4',*a*'-benzene-1,3,5-triyltris(benzoic acid) (H<sub>3</sub>BTB) ligands reacted with Cp<sub>2</sub>ZrCl<sub>2</sub> under similar synthesis conditions. Complexes **3** and **4** are cationic coordination tetrahedra, i.e., {[Cp<sub>3</sub>Zr<sub>3</sub>μ<sub>3</sub>-O(μ<sub>2</sub>-OH)<sub>3</sub>]<sub>4</sub>(BPDC)<sub>6</sub>}<sup>4+</sup> (ZrT-3) and {[Cp<sub>3</sub>Zr<sub>3</sub>μ<sub>3</sub>-O(μ<sub>2</sub>-OH)<sub>3</sub>]<sub>4</sub>(BTB)<sub>4</sub>}<sup>4+</sup> (ZrT-4), which are isostructures with **1** and **2**, respectively (Figure 2c,d and Table S2 in the SI). However, their packing modes in crystals of ZrT-3 and -4 are significantly different from those of ZrT-1 and -2, which crystallize in cubic

space groups of *Fm* $\bar{3}$ *m* and *F* $\bar{4}$ 3*m*, respectively. Moreover, the cubic phases of ZrT-3 and -4 are exceptionally less dense than the tetragonal phases of ZrT-1 and -2. In the crystal of **3**, there are eight ZrT-3 units per unit cell that stack edge-to-edge to form a simple cubic net (Figure S3a,c in the SI), and each unit cell contains one large truncated octahedral interstitial site in its center with 67.7% solvent-accessible volume. Compared with **3**, the crystal of **4** has the lower stacking density and the porosity is up to 74.1%. Furthermore, four ZrT-4 units in one unit cell are widely spaced and packed in face-centered-cubic mode, where the tetrahedral and octahedral pores are spontaneously created with a ratio of 2:1 (Figure S3b,d in the SI). Taken together, ZrT-1 and -4 show respectively the highest and lowest stacking densities among all four coordination tetrahedra, and the internal cavity volume and efficient window size increase with ligand extension.

Complexes **1–4** possess certain solubility in polar solvents such as methanol (MeOH) and dimethyl sulfoxide (DMSO), which can provide the possibility for ZrT-*X* as a kind of host molecule in supramolecular chemistry. Consequently, <sup>1</sup>H NMR and electrospray ionization mass spectrometry (ESI-MS) analyses of activated **1–4** were performed to determine their stability in solution. The <sup>1</sup>H NMR spectra of ZrT-1, -3, and -4 in DMSO-*d*<sub>6</sub> and ZrT-2 in MeOH-*d*<sub>4</sub> show very simple peaks and only one set of ligand proton resonances, which reflect the formation of discrete, highly symmetric coordination tetrahedra (Figure 3).

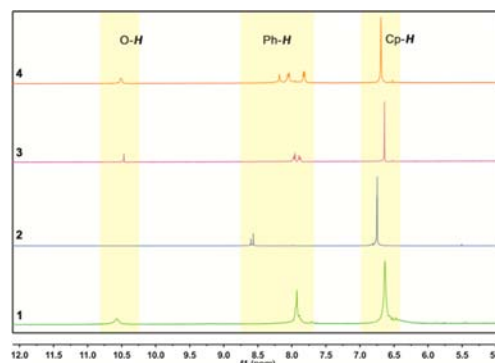


**Figure 3.** <sup>1</sup>H NMR spectra (400 MHz, 295 K, DMSO-*d*<sub>6</sub>) of **1**, **3**, and **4** and <sup>1</sup>H NMR spectra (400 MHz, 295 K, MeOH-*d*<sub>4</sub>) of **2** (**2** has poor solubility in DMSO-*d*<sub>6</sub>, so MeOH-*d*<sub>4</sub> was used).

As shown in the <sup>1</sup>H NMR spectrum of each tetrahedral assembly, the proton signals for the Cp and Ph groups respectively resonate in the ranges of 6.60–6.75 and 7.75–8.60 ppm, while the proton signals for the hydroxyl groups are at 10.45–10.60 ppm. It is worth noting that the proton signals for the BTC ligands in ZrT-2 are split into two sets of peaks (8.55 and 8.58 ppm) because of the two different tetrahedra in the solution with the ratio of 2:3 inferred from the integral. The major difference between the two tetrahedra is that one is empty and the other is occupied by a DMF molecule with large upfield-shifting signals of -0.46 and -1.66 ppm in <sup>1</sup>H NMR. This difference is also confirmed by ESI-MS analyses because of the two close signals (Figure S5 in the SI). Because the efficient window size of ZrT-2 is very small and is not effective enough to enable the guest DMF molecule to move freely in and out of the tetrahedral cage, DMF@ZrT-2 should form in the synthesis and exist in the crystal. However, the included DMF molecule cannot be located from difference maps because of partial occupancy and high symmetry. ESI-MS shows further evidence that the

tetrahedral assemblies remain intact in the solution, and the  $[M-2H^+ \cdot Cl^-]^+$  ions ( $M$  represents the intact assemblies  $ZrT-X$ ) locate at  $m/z$  3160.4, 3004.2, 3635.7, and 3936.5 for  $ZrT-X$  (Figures S4–S7 in the SI), respectively, which is consistent with a whole tetrahedron losing two  $H^+$  and three  $Cl^-$ . Meanwhile, the peaks attributable  $[M]^{2+}$ ,  $[M]^{3+}$ , and even  $[M]^{4+}$  for  $ZrT-X$  are also observed. Echoing the  $^1H$  NMR of  $ZrT-2$ , in the MS of  $ZrT-2$  the peaks appear in pairs with a difference of about  $m/z$  74 in the  $[M]^+$  mode, which can be attributed to a DMF molecule. Above all, the results of  $^1H$  NMR and ESI-MS clearly reveal that these coordination tetrahedra stably exist in solution, which offers the possibility for the study of supramolecular chemistry in solution.

Powder X-ray diffraction (PXRD) identified the phase purity of bulk samples for the four complexes (Figures S8–S11 in the SI). To determine whether these tetrahedral structures have architectural rigidity and permanent porosity after activation, we measured the  $N_2$ ,  $H_2$ , and  $CO_2$  adsorption isotherms of the four activated samples (Figures 4 and S13 and S14 in the SI). The

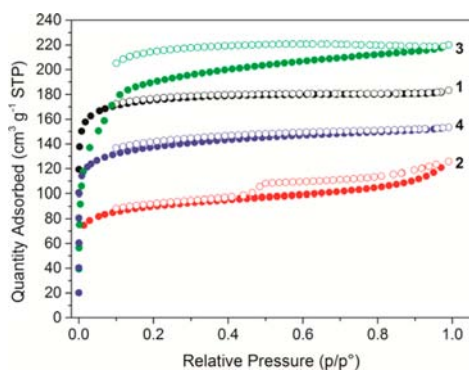


**Figure 4.**  $N_2$  sorption isotherms of activated 1–4. Solid and open circles represent adsorption and desorption data.

isotherm shapes of 1–4 are best described as type I or pseudo-type I with the apparent Brunauer–Emmett–Teller surface areas in the range of  $341\text{--}729\text{ m}^2\text{ g}^{-1}$  (Table S3 in the SI), and the slight hysteric behavior of 2 and 3 implies the presence of structural inhomogeneity or poor uniformity in the crystal size distribution. Furthermore, 1–4 adsorbed  $7.05\text{--}11.8\text{ mg g}^{-1}$  of  $H_2$  at 77 K and 1 bar and  $60.2\text{--}113\text{ mg g}^{-1}$  of  $CO_2$  at 273 K and 1 bar, in which some hysteresis was observed in the  $H_2$  and  $CO_2$  isotherms upon desorption (Table S3 in the SI). The results are similar to the ones with the cage structure in the literature. The permanent porosity of the hydrogen-bonding framework in the crystal structure has not been retained; however, the individual tetrahedral structure and porosity of 1–4 are maintained at the molecular level even in amorphous.<sup>2b,7</sup>

In summary, the coordination zirconocene tetrahedra represent new examples of tetrahedral cages, which provide a novel strategy for the synthesis of a tetrahedral assembly. The successful in situ synthesis of these coordination tetrahedra shows that the trinuclear zirconocene unit as a node is controllable and reproducible. We believe that the coordination zirconocene tetrahedra will become new study members of the supramolecular tetrahedral assembly and will derive some interesting chemistry.

## ■ ASSOCIATED CONTENT

### 📄 Supporting Information

Full experimental details, crystallographic analysis and crystal data (CIF), ESI-MS, PXRD, TGA, gas sorption, and additional figures and tables. This material is available free of charge via the Internet at <http://pubs.acs.org>.

## ■ AUTHOR INFORMATION

### Corresponding Author

\*E-mail: [ydq@fjirsm.ac.cn](mailto:ydq@fjirsm.ac.cn). Tel: +86-0591-83792525.

### Notes

The authors declare no competing financial interest.

## ■ ACKNOWLEDGMENTS

This work was supported by the NSFC (Grants 21271172 and 21131006), the “One Hundred Talent Project” from Chinese Academy of Sciences, and the NSF of Fujian Province (Grant 2012J01058).

## ■ REFERENCES

- (1) (a) Seidel, S. R.; Stang, P. J. *Acc. Chem. Res.* **2002**, *35*, 972–983. (b) Cook, T. R.; Vajpayee, V.; Lee, M. H.; Stang, P. J.; Chi, K. W. *Acc. Chem. Res.* **2013**, *46*, 10.1021/ar400010v. (c) Tranchemontagne, D. J.; Ni, Z.; O’Keeffe, M.; Yaghi, O. M. *Angew. Chem., Int. Ed.* **2008**, *47*, 5136–5147. (d) Yoshizawa, M.; Klosterman, J. K.; Fujita, M. *Angew. Chem., Int. Ed.* **2009**, *48*, 3418–3438. (e) Ke, Y.; Collins, D. J.; Zhou, H.-C. *Inorg. Chem.* **2005**, *44*, 4154–4156.
- (2) (a) Pluth, M. D.; Bergman, R. G.; Raymond, K. N. *Science* **2007**, *316*, 85–88. (b) Mal, P.; Breiner, B.; Rissanen, K.; Nitschke, J. R. *Science* **2009**, *324*, 1697–1699. (c) Ousaka, N.; Grunder, S.; Castilla, A. M.; Whalley, A. C.; Stoddart, J. F.; Nitschke, J. R. *J. Am. Chem. Soc.* **2012**, *134*, 15528–15537. (d) Custelcean, R.; Bonnesen, P. V.; Duncan, N. C.; Zhang, X.; Watson, L. A.; Van Berkel, G.; Parson, W. B.; Hay, B. P. *J. Am. Chem. Soc.* **2012**, *134*, 8525–8534. (e) Bilbeisi, R. A.; Clegg, J. K.; Elgrishi, N.; Hatten, X. d.; Devillard, M.; Breiner, B.; Mal, P.; Nitschke, J. R. *J. Am. Chem. Soc.* **2012**, *134*, 5110–5119. (f) Zarra, S.; Smulders, M. M. J.; Lefebvre, Q.; Clegg, J. K.; Nitschke, J. R. *Angew. Chem., Int. Ed.* **2012**, *51*, 6882–6885. (g) Liu, T.; Liu, Y.; Xuan, W.; Cui, Y. *Angew. Chem., Int. Ed.* **2010**, *49*, 4121–4124. (h) Sudik, A. C.; Millward, A. R.; Ockwig, N. W.; Cote, A. P.; Kim, J.; Yaghi, O. M. *J. Am. Chem. Soc.* **2005**, *127*, 7110–7118.
- (3) (a) Smulders, M. M. J.; Riddell, I. A.; Browne, C.; Nitschke, J. R. *Chem. Soc. Rev.* **2013**, *42*, 1728–1754. (b) Young, N. J.; Hay, B. P. *Chem. Commun.* **2013**, *49*, 1354–1379.
- (4) (a) Mirtschin, S.; Krasniqi, E.; Scopelliti, R.; Severin, K. *Inorg. Chem.* **2008**, *47*, 6375–6381. (b) Mishra, A.; Jung, H.; Lee, M. H.; Lah, M. S.; Chi, K. W. *Inorg. Chem.* **2013**, *52*, 8573–8578. (c) Shanmugaraju, S.; Vajpayee, V.; Lee, S.; Chi, K.-W.; Stang, P. J.; Mukherjee, P. S. *Inorg. Chem.* **2012**, *51*, 4817–4823. (d) Paul, L. E. H.; Therrien, B.; Furrer, J. *Inorg. Chem.* **2012**, *51*, 1057–1067. (e) Therrien, B. *Eur. J. Inorg. Chem.* **2009**, 2445–2453. (f) Huang, S. L.; Lin, Y. J.; Hor, T. S.; Jin, G. X. *J. Am. Chem. Soc.* **2013**, *135*, 8125–8128.
- (5) Boutonnet, F.; Zablocka, M.; Igau, A.; Jaud, J.; Majoral, J.-P.; Schamberger, J.; Erker, G.; Werner, S.; Krüger, C. *J. Chem. Soc., Chem. Commun.* **1995**, 823–824.
- (6) Spek, A. L. *J. Appl. Crystallogr.* **2003**, *36*, 7–13.
- (7) (a) Li, J.-R.; Zhou, H.-C. *Nat. Chem.* **2010**, *2*, 893–898. (b) Li, J.-R.; Zhou, H.-C. *Angew. Chem., Int. Ed.* **2009**, *48*, 8465–8468.